UC Irvine
UC Irvine Previously Published Works

Title

Very-long-range disynaptic V1 connections through layer 6 pyramidal neurons revealed by transneuronal tracing with rabies virus

Permalink

https://escholarship.org/uc/item/5196k02r

Journal

Eye and Brain, Volume 6(Thematic series: Organization and function of the visual system in primates)

ISSN

1179-2744

Authors

Liu, Yong-Jun
Arreola, Miguel
Coleman, Cassandra M
et al.

Publication Date

2014

DOI

10.2147/eb.s51818

Copyright Information

This work is made available under the terms of a Creative Commons Attribution-NonCommercial License, available at https://creativecommons.org/licenses/by-nc/4.0/

Peer reviewed

eScholarship.org Powered by the California Digital Library
University of California

Eye and Brain

Dovepress
open access to scientific and medical research

Open Access Full Text Article

ORIGINAL RESEARCH

Very-long-range disynaptic V1 connections through layer 6 pyramidal neurons revealed by transneuronal tracing with rabies virus

This article was published in the following Dove Press journal:
Eye and Brain
24 September 2014
Number of times this article has been viewed

Yong-Jun Liu
Miguel Arreola
Cassandra M Coleman
David C Lyon

Department of Anatomy and Neurobiology, School of Medicine, University of California, Irvine, CA, USA

Abstract: Neurons in primary visual cortex (V1) integrate across the representation of the visual field through networks of long-range projecting pyramidal neurons. These projections, which originate from within V1 and through feedback from higher visual areas, are likely to play a key role in such visual processes as low contrast facilitation and extraclassical surround suppression. The extent of the visual field representation covered by feedback is generally much larger than that covered through monosynaptic horizontal connections within V1, and, although it may be possible that multisynaptic horizontal connections across V1 could also lead to more widespread spatial integration, nothing is known regarding such circuits. In this study, we used injections of the CVS-11 strain of rabies virus to examine disynaptic long-range horizontal connections within macaque monkey V1. Injections were made around the representation of 5° eccentricity in the lower visual field. Along the opercular surface of V1, we found that the majority of connected neurons extended up to 8 mm in most layers, consistent with twice the typically reported distances of monosynaptic connections. In addition, mainly in layer 6, a steady presence of connected neurons within V1 was observed up to 16 mm away. A relatively high percentage of these connected neurons had large-diameter somata characteristic of Meynert cells, which are known to project as far as 8 mm individually. Several neurons, predominantly in layer 6, were also found deep within the calcarine sulcus, reaching as far as 20° of eccentricity, based on estimates, and extending well into the upper visual field representation. Thus, our anatomical results provide evidence for a wide-ranging disynaptic circuit within V1, mediated largely through layer 6, that accounts for integration across a large region of the visual field.

Keywords: visual cortex, horizontal connections, long-range lateral connections, Meynert cells, surround suppression, feedback

Introduction

In primary visual cortex (V1), pyramidal neurons send axons laterally, forming an extensive horizontal lattice of connectivity within the superficial and deep layers.[1–6] In higher visual species such as carnivore, primate, and tree shrew, horizontal connections are strikingly patchy and link together neurons found in similar orientation columns,[7–13] providing a network that may lead to facilitation of responses at low stimulus contrast[14–17] and enhanced selectivity to stimulus orientation.[16,18–20] In addition, because long-range lateral connections can integrate across the visual field representation, they are capable of providing a global context important for processing of visual scenes.[21–24] One such process studied extensively in both monkey and cat is that of extraclassical surround suppression,[15,16,19,23,25–29] which may be mediated indirectly through long-range lateral connections originating from excitatory pyramidal cells synapsing onto local inhibitory neurons,[13,30–32] or even directly through a subtype of

Correspondence: David C Lyon
Department of Anatomy and Neurobiology, School of Medicine, 364 Med Surge II, University of California, Irvine, CA 92697-1275, USA
Tel +1 949 824 0447
Fax +1 949 824 8549
Email dclyon@uci.edu

© 2014 Liu et al. This work is published by Dove Medical Press Limited, and licensed under Creative Commons Attribution – Non Commercial (unported, v3.0) License. The full terms of the License are available at http://creativecommons.org/licenses/by-nc/3.0/. Non-commercial uses of the work are permitted without any further permission from Dove Medical Press Limited, provided the work is properly attributed. Permissions beyond the scope of the License are administered by Dove Medical Press Limited. Information on how to request permission may be found at: http://www.dovepress.com/permissions.php

long-range projecting inhibitory neurons.[33] However, the role of intrinsic V1 connections in surround suppression has been called into question.[15,34–36] This is because, even though long-range connections typically extend up to 3–4 mm, the region of visual space covered in V1 is relatively small compared to the full extent of the extraclassical surround.[12,14,37]

Instead of long-range lateral connections, feedback from higher visual areas has been proposed as a more likely source of inputs to the full extraclassical surround, since the extent of the visual field representation covered by feedback is generally much larger.[14,38] Through this circuit, surround suppression could be mediated via excitatory feedback projections synapsing onto local inhibitory neurons,[39] for which there is anatomical support, although the occurrence of feedback neurons synapsing onto local inhibitory cells is significantly lower than onto local excitatory neurons.[40–42] Nevertheless, it is just as possible that the full extent of the extraclassical surround could be covered by a string of multisynaptic long-range lateral connections within V1.

In this study, we used a transneuronal rabies virus and limited the transport time to 72 hours to determine the extent of intrinsic V1 connections across two synapses. We found that the majority of connected neurons extended up to 8 mm in layers 2/3, 4A, 4B, 5, and 6, consistent with twice the typically reported distances of monosynaptic connections.[6,14] An additional, steady presence of neurons was found up to 16 mm away, most prominently in layer 6. Moreover, several neurons, also predominantly in layer 6, were found deep within the calcarine sulcus. A relatively high percentage of these long-range layer 6 neurons had large cell body sizes characteristic of Meynert cells[43–46] – cells that can project as far as 8 mm individually.[47] Our anatomical results show that a disynaptic horizontal network within layer 6 is capable of reaching at least twice as far as the previously reported maximum distance for monosynaptic Meynert cell projections, allowing for integration across a large region of the visual field independent of feedback from higher visual areas.

Methods

Surgical procedures

One adult male macaque monkey was used following procedures approved by the Salk Institute Animal Care and Use Committee. Procedures involving rabies virus were conducted using biosafety level 2 precautions as described elsewhere.[48]

The animal was anesthetized as previously described[49] and placed in a stereotaxic head frame. Under sterile conditions, the dorsolateral surface of V1 of the right hemisphere was exposed, and injections of the challenge virus strain-11 ([CVS-11] see Rabies virus strain and speed of transport section) of rabies virus were made at six locations spaced ~2 mm apart, forming a 2×3 grid just lateral to the medial lip in a region corresponding to ~5° of eccentricity in the lower visual quadrant (see Figure 1). At each location, 0.3 μL of rabies virus was injected at three depths spaced by 0.7 mm (0.7, 1.4, and 2.1 mm deep) using a glass pipette (tip diameter ~30 μm) attached to a Pneumatic Pico Pump (PV820; World Precision Instruments, Sarasota, FL, USA). Injections were placed first at the deepest penetration (2.1 mm) and then moved upward toward the surface for the subsequent injections.

Rabies virus strain and speed of transport

A 72-hour survival time following injections of the CVS-11 strain of rabies virus into V1 was used to allow disynaptic retrograde transport. Different preparations of rabies virus spread through the nervous system at different rates depending on the passage history of the virus.[48,50,51] The CVS-11 rabies virus strain that we used here was passaged four times in mouse brain, followed by five times in cultured chicken embryo-related cells, and had a titer of 1×10^4 plaque-forming units (PFU)/mL (supplied by Dr Donald Lodmell, National Institutes of Health/National Institute of Allergy and Infectious Diseases, Rocky Mountain Laboratory, Hamilton, MT, USA). The titer of our virus (~1×10^7 PFU/mL) was lower than that of the CVS-11 virus used by Kelly and Strick,[52] who confirmed that a 72-hour survival time limited infection to second-order neurons. Similar controls for our lower-titer virus were used in three previous publications.[49,53,54] Therefore, it is highly unlikely that our lower-titer virus would have infected beyond two synapses.

Histology

After the 72-hour survival time, the animal was sacrificed and perfused transcardially, first with saline and then with 4% paraformaldehyde in phosphate buffer (pH 7.4). The brain was removed, then postfixed and cryopreserved overnight in 4% paraformaldehyde and 30% sucrose in phosphate buffer. The brain was then kept in 30% sucrose without 4% paraformaldehyde for another 5 days. Brain sections were cut coronally at 40 μm on a freezing microtome. Every sixth section was processed for cytochrome oxidase (CO),[55] and then for the rabies nucleocapsid protein to reveal rabies virus-infected neurons. For this, immunohistochemistry was performed using the anti-nucleocapsid mouse monoclonal antibody (gifted by Dr Donald Lodmell) and the biotinylated horse anti-mouse secondary antibody (Vector Labs, Burlingame,

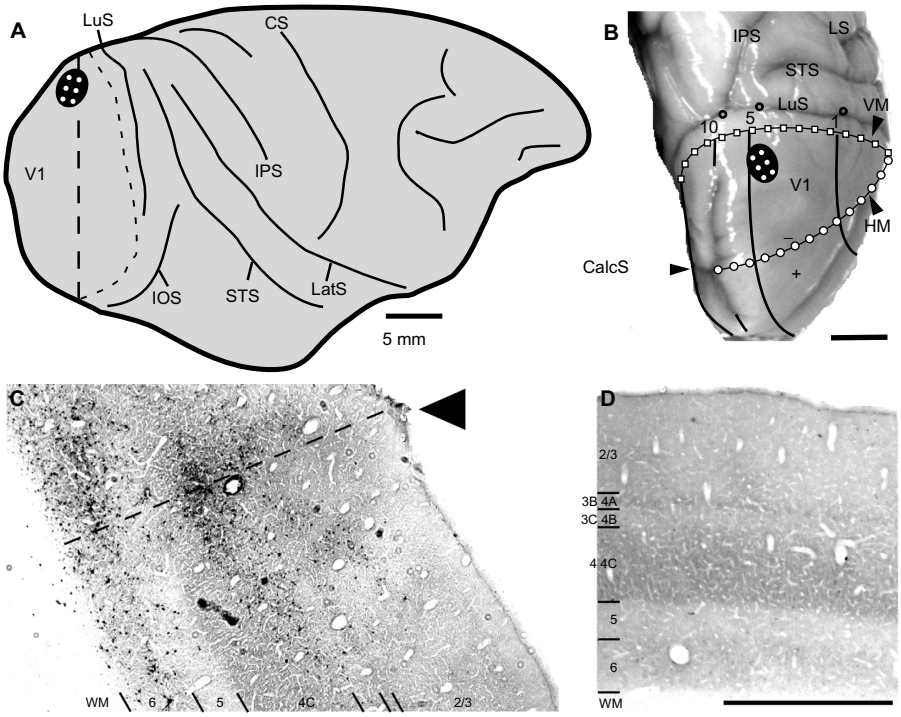

Figure 1 Rabies virus injections in macaque monkey primary visual cortex.

Notes: (**A**) Locations of the V1 injection sites (white dots within the black oval) are shown on a drawing of the dorsal lateral view of the right hemisphere of the adult male macaque monkey. The approximate location of the V1/V2 border is indicated by the curved dashed line just posterior to the LuS. (**B**) An image from a representative brain shows a dorsal view of the posterior end of cortex. The representations of the HM and VM and iso-eccentricities of 1°, 5°, and 10° are based on Lyon and Kaas,[83] and were derived from retinotopic maps provided in Van Essen et al[59] and Weller and Kaas.[60] The digital image in (**C**) shows one of the V1 injection sites. The image was taken from a coronal section through the plane indicated by the vertical dashed line in (**A**). Rabies-infected neurons are stained black from immunohistochemistry of the rabies nucleocapsid protein. The arrowhead points to a perturbation on the cortical surface caused by insertion of the injection pipette. The diagonal dashed line estimates the path of the injection pipette. Cortical layers were determined from cytochrome oxidase staining patterns (see also [**D**]), and are indicated at the bottom of the image. (**D**) A digital image of a cytochrome oxidase-stained coronal section shows the V1 lamination in greater detail. Gray text to the left shows the terminology of Hassler,[85] as an alternative to the terminology of Brodmann,[56] which is shown in black. The scale bars in (**A**) and (**B**) are 5 mm. The scale bar in (**D**) is 1 mm and also applies to (**C**).

Abbreviations: CalcS, calcarine sulcus; CS, central sulcus; HM, horizontal meridian; IOS, inferior occipital sulcus; IPS, intraparietal sulcus; LatS, lateral sulcus; LuS, lunate sulcus; STS, superior temporal sulcus; V1, primary visual cortex; V2, secondary visual cortex; VM, vertical meridian; WM, white matter.

CA, USA) and revealed through a diaminobenzidine reaction. V1 was identified through distinct CO staining patterns, including a thick, CO dark layer 4C (using the terminology of Brodmann[56]), corresponding to the main geniculate input layer, and a thin, CO dark layer 4A (see Figure 1D).

Data analysis

Every 24th section throughout the entire V1 region, and every 12th section near the injection sites, was examined for rabies-labeled neurons. Infected neurons were identified and plotted under bright-field illumination using a Zeiss Axioplan microscope (Carl Zeiss Microscopy GmbH, Jena, Germany) at low magnification (×10 objective, 0.45 NA) and a high-power digital camera (Cooke SensiCam QE; PCO-TECH Inc., Romulus, MI, USA) to send live images to a Neurolucida computerized reconstruction system (MBF Bioscience, Williston, VT, USA). Reconstructions of the laminar boundaries of V1 were aided by CO staining of the same sections that were stained for rabies nucleocapsid (for examples, see Figures 1C, 2, and 3). In every section, cell counts were made for each layer and the number multiplied by 12 or 24 to provide an interpolated count, since one in 12 (near injection sites) or one in 24 sections were sampled. The distance of each neuron from the lateralmost or medialmost injection sites were also determined at 0.5 mm increments for neurons found on the opercular surface and immediately adjacent along the medial wall (see examples of distance measurements in Figure 3A). Note that, because rabies virus does not leave an injection-site halo,[57] the uptake region from each injection site was estimated to have a radius of 0.5 mm. The distance of each counted neuron is relative to this estimated edge of the injection, not to the center of the injection track.

Pyramidal neurons with cell somata >30 μm in diameter were labeled as "large" cells and identified within Neurolucida using an open circular curser size set to a 30 μm diameter; cells <30 μm were considered "small". The 30 μm diameter was chosen as a conservative estimate of layer 6 Meynert cells and is based on previous reports showing that their average diameter is 22.3 μm, whereas the typical

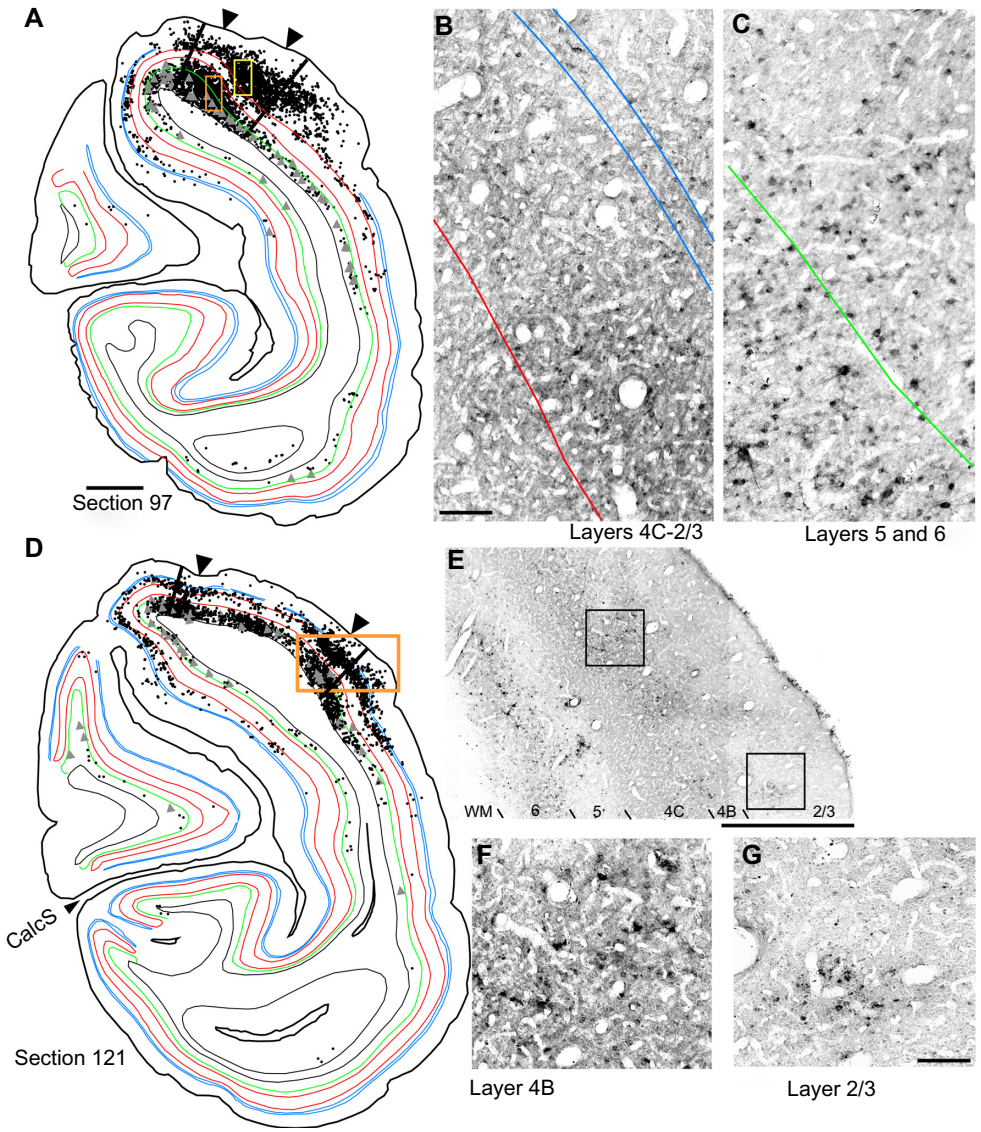

Figure 2 The distribution of rabies-infected neurons in two coronal sections of V1 of the right hemisphere.
Notes: (**A**) A reconstruction of section 97 shows portions of two rabies virus injection sites (black arrowheads). Neurons retrogradely labeled from these injections are shown as small black dots or large gray triangles depending on whether or not they were larger than 30 μm in diameter. The parallel blue lines represent the upper and lower border of layer 4A (Hassler's layer 3B[84]); parallel red lines represent the upper and lower border of layer 4C (Hassler's layer 4[84]); and the green line represents the layer 5/6 border. The thick black line indicates the cortical surface, and the thin black line represents the border between white matter and layer 6. The digital image in (**B**) shows layers 4C-2/3 and is from the region in (**A**) outlined by the yellow rectangle. The digital image in (**C**) shows layers 5 and 6 and is from the region in (**A**) outlined by the orange rectangle. (**D**) A reconstruction of section 121 shows portions of two rabies virus injection sites indicated by black arrowheads. The digital image in (**E**) shows rabies-infected neurons throughout layers 2/3-6, and is from the inset region outlined in (**D**) by the orange rectangle. Enlarged views of the layer 4B and layer 2/3 regions outlined by left and right black squares, respectively, in (**E**) are shown in (**F**) and (**G**). The scale bar in (**A**) is 2 mm and also applies to (**D**). The scale bar in (**E**) is 1 mm. Scale bars in (**B**) and (**G**) correspond to 100 μm and also apply to (**C**) and (**F**).
Abbreviations: CalcS, calcarine sulcus; V1, primary visual cortex; WM, white matter.

diameter of all other pyramidal neuron somata (in primary visual cortex) is around 13 μm.[43] Even though large diameters can be useful for identifying Meynert cells, not all Meynert cells necessarily have large cell bodies.[58] Therefore, our numbers of this cell type based on cell body diameter alone is likely to be an underestimate. In addition to layer 6 Meynert cells, we also identified a relatively small number of large-diameter pyramidal neurons in layer 4B, likely corresponding to Meynert–Cajal cells as reported by others.[45,46]

Digital images shown in Figures 1–3 were captured by the Cooke SensiCam and were cropped and adjusted for brightness and contrast in Canvas software (version 11; ACD Systems International Inc., Seattle, WA, USA). None of the images was altered in any other way.

Results

To determine the extent of disynaptic long-range lateral connections within V1, we made several injections of the CVS-11

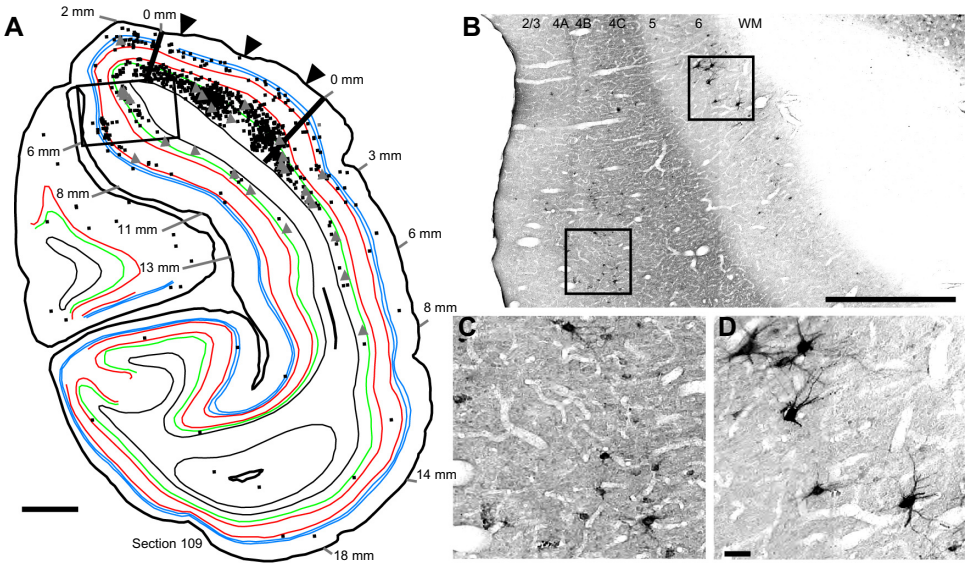

Figure 3 The distribution of rabies-infected neurons in a single cross-section of V1 of the right hemisphere.
Notes: (**A**) A reconstruction of section 109 shows portions of three rabies virus injection sites (black arrowheads). Neurons retrogradely labeled from these injections are shown as small black dots or large gray triangles. The two solid black lines adjacent to the medial and lateral injection sites represent the starting point (0 mm) for the calculations of all connected neurons along the opercular surface, laterally, and the medial wall, medially. Distances of up to 18 mm are indicated. The digital image in (**B**) shows rabies-infected neurons in layers 2/3-6 in V1 and is from the inset region outlined in (**A**) by the black rectangle. An enlarged view of a cluster of small layer 4A and 4B rabies-infected neurons is shown in (**C**), and is taken from the area outlined by the left square in (**B**); An enlarged view of a cluster of large layer 6 neurons, all with cell body diameters >30 μm, is shown in (**D**), and is taken from the area outlined by the right square in (**B**). The scale bars in (**A**), (**B**), and (**D**) are 2 mm, 1 mm, and 50 μm, respectively. The scale bar in (**D**) also applies to (**C**).
Abbreviations: V1, primary visual cortex; WM, white matter.

strain of rabies virus within a small 2×3 grid, covering 2×4 mm on the dorsal lateral surface of V1 in one hemisphere of a macaque monkey (Figure 1A). The injected region was estimated to be just within 5° of the lower visual field representation, nearer to the vertical meridian (Figure 1B). An example of rabies virus infection near one of the injection sites is shown in Figure 1C, where dense clusters of rabies-infected neurons are visible in layers 2/3–6. Note that, unlike traditional neuronal tracers, rabies virus does not leave a halo, making injected locations less prominent.[57] Nevertheless, this site could be verified based on the surface perturbation caused by the needle insertion and the denser clusters of infected neurons.

Reconstructions of entire coronal sections containing parts of several of the injection sites (black arrowheads) are shown in Figures 2 and 3. In each of these 40 μm-thick sections, which are composed almost entirely of V1, retrogradely connected neurons, while far more numerous within a few millimeters of the injections, are nevertheless found throughout the extent of V1, including along the lateral pole more than 18 mm away and within the lower bank of the calcarine sulcus. Infected neurons located nearer to the injection sites are more likely to represent both mono- and disynaptically labeled neurons, whereas neurons located further from the injection site are increasingly more likely to represent disynaptically labeled neurons. This is especially the case for neurons found further than 4 mm or 8 mm away, which represent the longest range reported for monosynaptic lateral connections in V1[6,14,47] for layers 2–5 and layer 6, respectively (see "Discussion"). Examining the laminar distributions, infected neurons were found at long range in all layers, but had a distinctive presence in layer 6 (Figures 2 and 3 [green line indicates the layer 5/6 border]), particularly beyond 4 mm. Also notable was the prevalence of neurons with relatively large-diameter somata in layer 6 (Figures 2A and D and 3A [displayed as gray triangles]), compared to other layers. For example, the cell bodies of the layer 6 pyramidal neurons shown in Figure 3D are each over 30 μm in diameter, more than twice the diameter of most neurons found in more superficial layers (Figure 3C). Based on their large size and laminar position, these neurons can be classified as Meynert cells (see "Methods" and "Discussion").

To examine the laminar pattern of long-range connections throughout more than 450 coronal sections containing V1, the position of every rabies-infected neuron was plotted for every 24th section (960 μm intervals). Near the injection sites, every 12th section was analyzed (sections 85–157). In all, infected V1 cells were found in 24 sections spanning over 20 mm from anterior to posterior. A sample of these sections is shown in Figure 4, where V1 can be distinguished

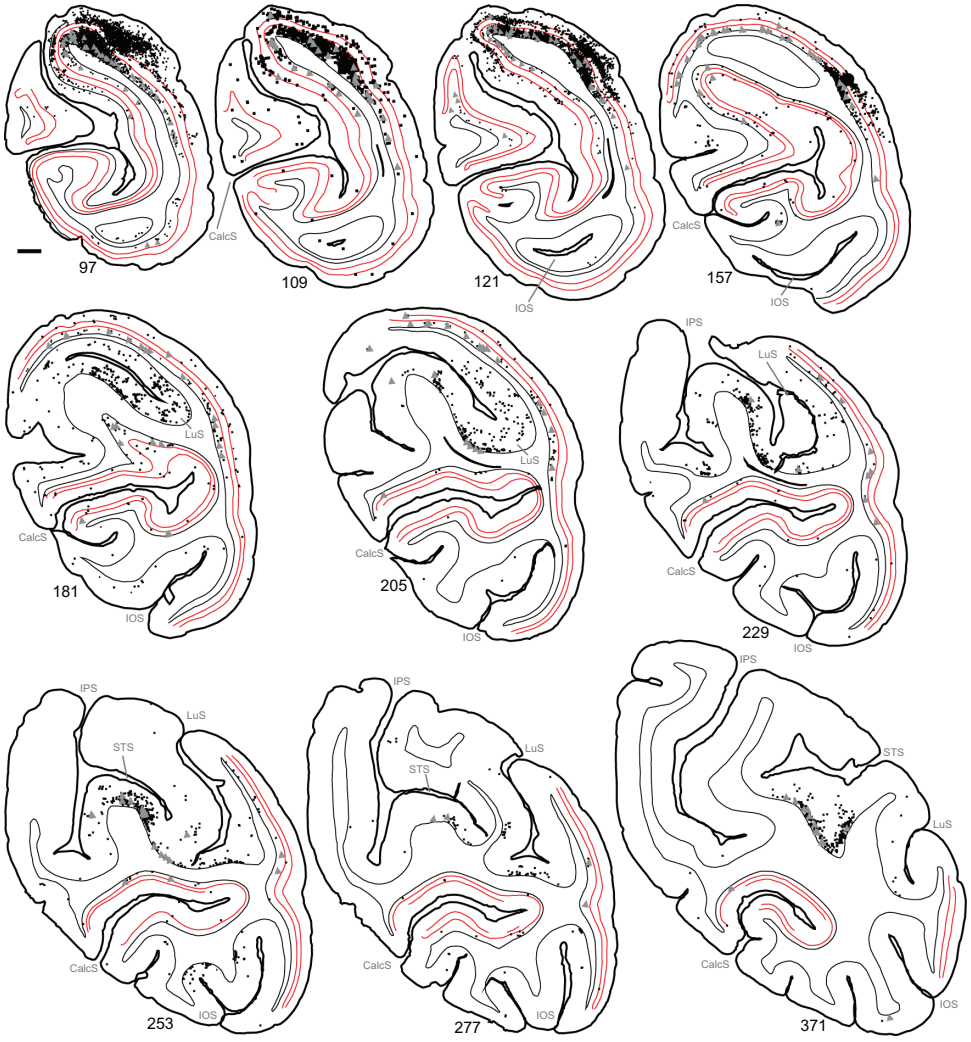

Figure 4 Serial reconstructions show the pattern of mono- and disynaptically connected neurons in visual cortex following rabies virus injections in V1.
Notes: Ten coronal sections are shown in order by rows, ranging from the most posterior (top left section) to the most anterior (bottom right section). Section numbers are listed to the lower left of each section and range from section 97 to section 371. Retrogradely infected neurons (black dots and gray triangles) were found in striate (V1) and extrastriate visual cortex. Red parallel lines representing layer 4C are used to delineate V1. Black dots = small neurons and gray triangles = large neurons. The relevant sulci are given in gray lettering. The scale bar shown for section 97 equals 2 mm and applies to all sections.
Abbreviations: CalcS, calcarine sulcus; IOS, inferior occipital sulcus; IPS, intraparietal sulcus; LuS, lunate sulcus; STS, superior temporal sulcus; V1, primary visual cortex.

by the parallel red lines used to delineate layer 4C. The relative distance of each labeled neuron from the lateral- and medial-most injection sites was determined for neurons located along the opercular surface and medial wall. For detailed examples of cell distances from the medial- and lateralmost injection sites, refer to section 109 shown in Figure 3A. The results of this analysis are given for different layers in Figure 5. In layers 2/3, 4B, and 6, there is a large number of neurons within the first 0.5 mm, ~3,200 in layer 6, and ~1,200–1,600 in layers 4B and 2/3, respectively (Figure 5A, C and F). The number gradually declines to about 400 cells in each of these three layers at around 3.5–4 mm, then plateaus somewhat until about the 8 mm mark. In the remaining layers, the number of neurons is fewer, but also extends to 4 mm for layer 4A (Figure 5B) and to 8 mm for layers 4C and 5 (Figure 5D and E). Beyond 8 mm, especially within layer 6, a number of connected neurons within V1 were observed up to 16 mm away (Figure 5F). A relatively high number of very-long-range layer 6 neurons had large somata (Figure 5L) characteristic of Meynert cells.[43–46] These large-diameter neurons were virtually absent from all other layers except for a sporadic distribution in layer 4B (Figure 5I).

The laminar position of infected neurons found in the calcarine sulcus was also tabulated. For these cells, distances from the injection sites were not considered because of the difficulties in knowing the direct paths taken through the convolutions of the calcarine sulcus. Nevertheless, cells in the calcarine can be considered to be further than 8 mm away, based on the distance shown in Figure 3A.

Figure 6 graphs the interpolated numbers of cells found in the calcarine sulcus and their distribution across layers. The most neurons were found in layer 6 (n=5,904). Fewer cells were found in layer 4B (n=2,928) and in layer 5 (n=1,248), with fewer still in layers 2/3 (n=432), 4A (n=264), and 4C (n=144). In layer 6, 26% of the infected neurons had somata over 30 μm in diameter, whereas in the only other layer with such large cells, layer 4B, these cells made up 5% of the labeled population.

Using the full series of reconstructions, we made an estimate of the range of the visual field representation covered in V1. This estimate was based on the detailed receptive field maps provided by Van Essen et al[59] and Weller and Kaas[60] that could be easily related to identifiable landmarks within the calcarine sulcus and along the opercular surface. As shown in Figure 7, stemming from the injection at ~5° eccentricity in the lower visual field, disynaptic connections within V1 spanned 2°–20° of the visual field, and were found well within the upper field representation. Cells corresponding to the 20° representation of the visual field were found more than halfway through the anterior–posterior extent of the calcarine sulcus, on both the upper (lower visual field representation) and lower (upper field) banks of the calcarine (see sections 229–371 in Figure 4). As noted above, most of these cells are located in layer 6 and several of them have large-diameter somata characteristic of Meynert cells (large gray triangles in Figure 4). Similarly, cells found most anteriorly on the opercular surface, near the representation of 2° in eccentricity, are shown in section 277 (Figure 4), are mainly found in layer 6, and are similar in size to Meynert cells (see also Figure 5L).

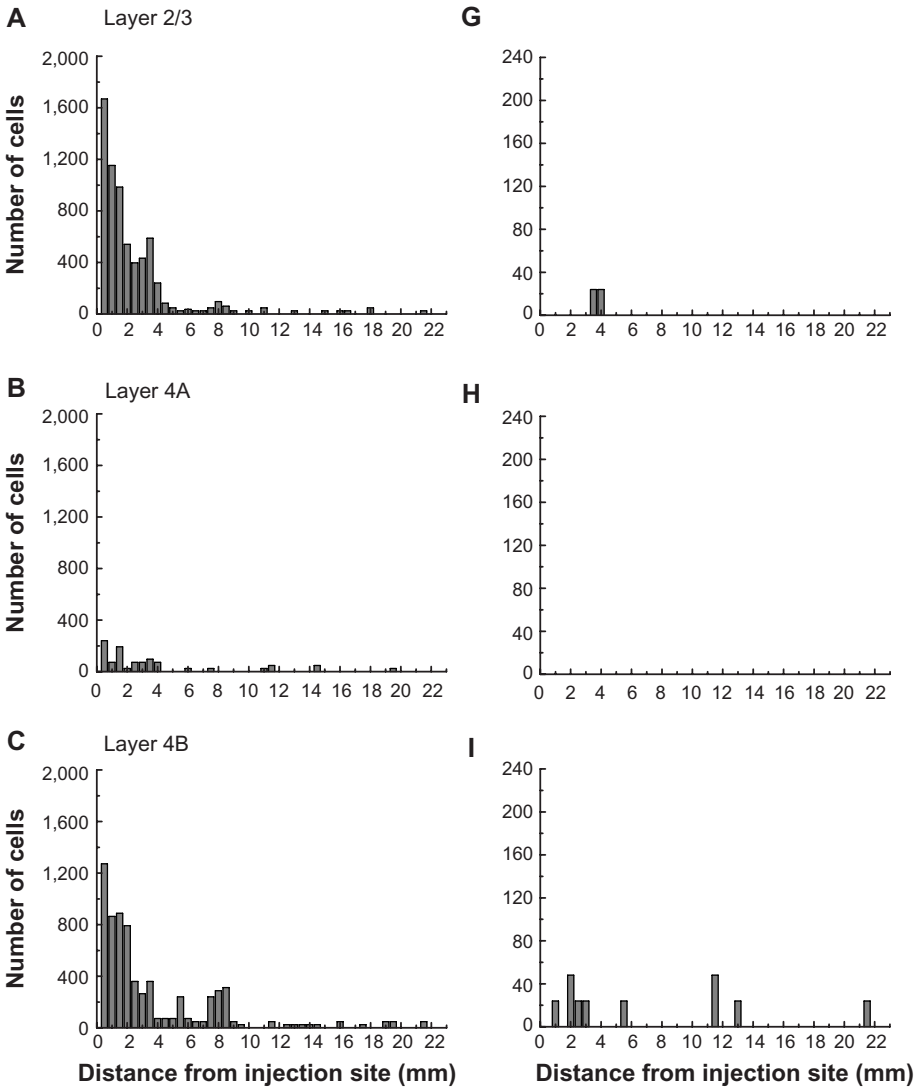

Figure 5 (*Continued*)

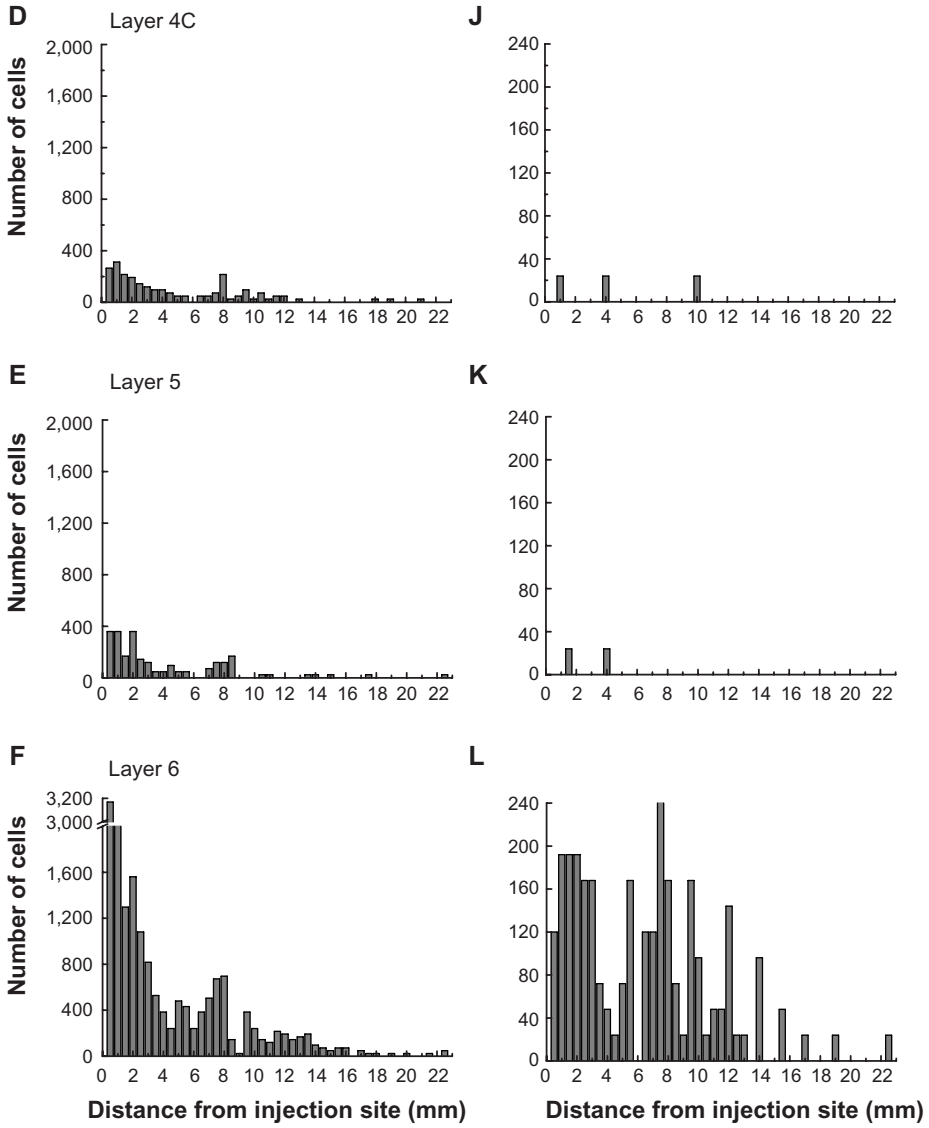

Figure 5 The numbers of retrogradely infected neurons found across several millimeters of the opercular surface of primary visual cortex.
Note: Small and large cells are graphed together in the left-hand panels (**A**–**F**), whereas large cells only are graphed in the right-hand panels (**G**–**L**).

Discussion

By using the CVS-11 strain of rabies virus as a transneuronal tracer, we were able to determine the length and laminar distribution of disynaptic long-range horizontal connections within macaque monkey V1. We found that the number of connected neurons in all layers was highest within 0.5 mm of the injection site and steadily declined over the first 4 mm. Between 4 and 8 mm, fewer neurons were found in most layers, but the number of cells in layer 6 remained relatively high. Beyond 8 mm, a steady presence of connected neurons was observed up to 16 mm away, primarily in layer 6. Between 4 and 16 mm, a relatively high percentage of these layer 6 neurons had large soma sizes characteristic of Meynert cells.[43–46] Several neurons, the majority of which were in layer 6, were also found deep within the calcarine sulcus, reaching as far as 20° in eccentricity and extending well into the upper visual field representation. These anatomical results provide evidence for a far-ranging disynaptic circuit within V1, mediated in large part through layer 6, that accounts for integration across a wide expanse of the visual field.

While we are unable to differentiate monosynaptic from disynaptic long-range lateral connected neurons, previous work using traditional monosynaptic tracers indicates that long-range connected neurons are typically found up to 3–4 mm from the injection site,[6,14,37] with a subpopulation of layer 6 Meynert cells projecting as far as 8 mm.[47] Therefore, the densest connectivity within the first 4–8 mm in our results is largely consistent with monosynaptic connectivity

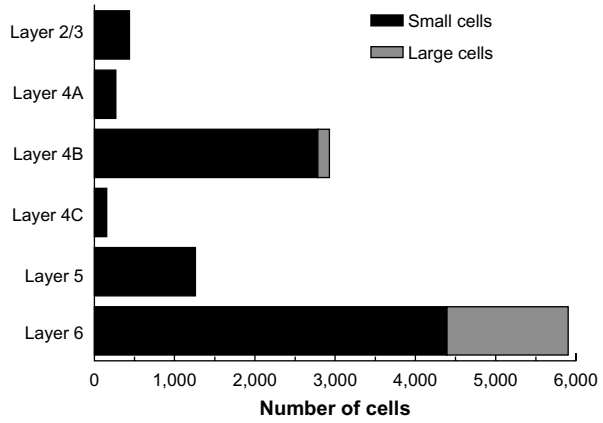

Figure 6 The numbers of retrogradely infected V1 neurons present in the calcarine sulcus.
Note: The proportions of large cells, which were present in layer 4B (5%) and layer 6 (26%), are indicated by gray shading.
Abbreviation: VI, primary visual cortex.

(0–4 mm), and subsequent disynaptically labeled inputs (4–8 mm) to these monosynaptically connected neurons, with some of the neurons between 4 and 8 mm likely being monosynaptically labeled Meynert cells. In contrast, the sparser labeling of neurons between 8 and 16 mm likely reflects disynaptic rabies virus infection only and should involve the longer-range projecting Meynert cells, as either the first- and/or second-order neuron infected. Indeed, of the putative disynaptically connected neurons found further than 8 mm away, most were located in layer 6, and a high proportion were identified as Meynert cells based on their large cell body diameter (Figures 5L and 6).

An alternative, or additional, explanation could be that these longer-range (>8 mm away) layer 6 neurons were infected through a feedback loop between higher visual areas, such as the middle temporal visual area (MT), to which layer 6 neurons project.[44,54,58,61] While there is no direct evidence for such a disynaptic circuit, this may help explain the handful of neurons found even further away than 16 mm. With our tracing approach, there is no way to rule out this alternative. Nevertheless, the documented distance of up to 8 mm for lateral axon projections of layer 6 Meynert cells[47] correlates well with a disynaptic explanation of the ~16 mm we observed in layer 6.

The significance of this very-long-range disynaptic circuit is that, through V1 alone, the full extent of the extraclassical surround is covered. That is, while 3–4 mm-long projections make up the majority of the horizontal connections and can be tied only to the small, "near" component of the extraclassical surround (see[14–16]), the longer projections of up to 8 mm reported for layer 6 Meynert cells,[47] and the very long disynaptic projections we find here, cover up to four times that of the near surround. Accordingly, these disynaptic projections covered 2°–20° of the visual field (Figure 7), comparable to the visual field range covered by feedback.[14] This is not to say that feedback connections do not also play a role in surround modulation of V1 neurons. There is both a fast[62,63] and a slower[19,27,63] emerging component of the surround. Long-range lateral connections are unmyelinated, therefore the signal transmits too slowly[64–66] (~0.1–0.2 mm/millisecond) to account for early effects,[62]

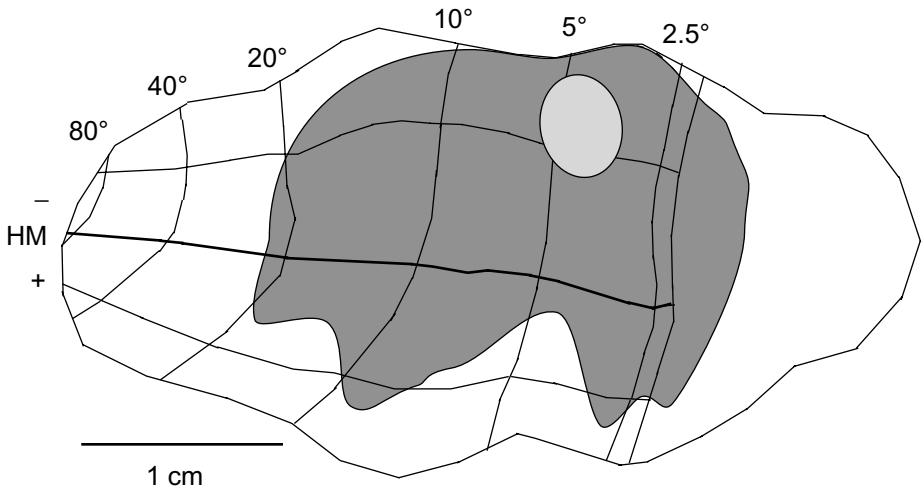

Figure 7 The region of visual space covered by the very-long-range disynaptic connections is shown on an unfolded, two-dimensional view of the V1 surface.
Notes: Iso-eccentricity contours from 2.5° to 80° and the HM are shown, and are based on the summary of V1 retinotopy provided in Van Essen et al.[59] The light gray oval represents the injection sites. The dark gray shading represents the spread of rabies-labeled neurons found for layer 6. The spread for layer 5 and for layers superficial to layer 4C were less extensive and are not shown. Upper and lower visual fields are indicated by + and –, respectively. The scale bar is 1 cm.
Abbreviations: HM, horizontal meridian; V1, primary visual cortex.

although the larger-diameter axons of Meynert cells[61] could potentially propagate signals faster. Surround effects within the first 20 milliseconds are most likely mediated through faster feedforward[63,67] and feedback circuits.[14,15,62] In contrast, the slower surround component builds in strength over 70 milliseconds or more and is consistent with long-range lateral connections arising from mono- or disynaptic distances over 7 mm.[19]

Consistent with our anatomical results, neurophysiological recordings have found that some layer 6 neurons in cat and monkey V1 integrate across a wider visual field representation than other neurons in more superficial layers.[25,27,68–72] For example, we recently showed that ~20% of infragranular layer neurons respond maximally to drifting grating apertures as large as 30° – significantly larger than other neurons within the same cortical columns by more than 3 times (see Figure 6 Liu et al[27]). The cells' preference for this large stimulus was a result of a facilitative surround that emerged slowly, over a 100-millisecond time window, more consistent with slower propagation speeds of long-range lateral connections than faster feedback from higher visual areas. Within layer 6, therefore, long-range disynaptic connections between excitatory Meynert cells may be feeding this slowly emerging facilitative surround. In contrast, this integration across visual space in layer 6 may lead to later emerging suppression for neurons found in other layers.[27] For example, when layer 6 neurons in cat and mouse V1 are inactivated, this leads to a net excitatory effect on more superficial neurons;[73–76] however, others have found the opposite effect for certain superficial layer cell types, such as hypercomplex cells,[77] in which responses are attenuated by layer 6 inactivation. Exactly what type of impact layer 6 has on different superficial cell types, and whether or not these ascending circuits are a part of this very-long-range lateral network we observed in macaque monkey V1, remains to be determined.

In a wide range of species, V1 neurons in layer 6 consist of several subtypes and are involved in numerous circuits, providing inputs to the lateral geniculate nucleus, pulvinar, claustrum, the reticular formation, superficial cortical layers within the cortical column, and higher visual areas (reviewed Thomson[78]). While several of these cell types are likely to be involved in long-range lateral connections, Meynert cells may play a highly specialized role. In primates, for example, Meynert cells are the only layer 6 cells that project to MT,[44,58] providing direction-selective inputs[79] to this motion-sensitive region.[80,81] Though not demonstrated in the same neurons, the direction selectivity of Meynert cells[79] and their potential to integrate over a wide expanse of the visual field[47] has led some to speculate that such cells serve as an anatomical substrate for predator detection.[82] Consistent with this idea, many of the same MT-projecting Meynert cells also send axon collaterals to the superior colliculus[44,58] that are likely to contribute to visually guided search behavior. In addition, layer 6 Meynert cells are implicated in the most direct feedforward relay of magnocellular and parvocellular inputs from the LGN to the MT.[54] This convergence of magno- and parvocellular inputs early in V1, and subsequent direct projection to the MT, may be instrumental in relaying a quick signal that covers a more complete range of spatial, temporal, luminance, and chromatic contrasts provided by the two LGN cell types, thus enhancing the effectiveness of a global early warning system.

Acknowledgments

We thank Dr Ed Callaway and the Salk Institute for generously providing the monkey and laboratory space for the rabies virus injection; Dr Jonathan Nassi for assistance with virus injections; and Dr Donald Lodmell for providing the CVS-11 strain of rabies virus and antibodies to the rabies nucleocapsid.

Disclosure

The authors report no conflicts of interest in this work.

References

1. Gilbert CD, Wiesel TN. Clustered intrinsic connections in cat visual cortex. *J Neurosci.* 1983;3(5):1116–1133.
2. Lyon DC, Jain N, Kaas JH. Cortical connections of striate and extrastriate visual areas in tree shrews. *J Comp Neurol.* 1998;401(1):109–128.
3. Rockland KS. Anatomical organization of primary visual cortex (area 17) in the ferret. *J Comp Neurol.* 1985;241(2):225–236.
4. Rockland KS, Lund JS. Widespread periodic intrinsic connections in the tree shrew visual cortex. *Science.* 1982;215(4539):1532–1534.
5. Rockland KS, Lund JS. Intrinsic laminar lattice connections in primate visual cortex. *J Comp Neurol.* 1983;216(3):303–318.
6. Yoshioka T, Blasdel GG, Levitt JB, Lund JS. Relation between patterns of intrinsic lateral connectivity, ocular dominance, and cytochrome oxidase-reactive regions in macaque monkey striate cortex. *Cereb Cortex.* 1996;6(2):297–310.
7. Bosking WH, Zhang Y, Schofield B, Fitzpatrick D. Orientation selectivity and the arrangement of horizontal connections in tree shrew striate cortex. *J Neurosci.* 1997;17(6):2112–2127.
8. Gilbert CD, Wiesel TN. Columnar specificity of intrinsic horizontal and corticocortical connections in cat visual cortex. *J Neurosci.* 1989;9(7):2432–2442.
9. Malach R, Amir Y, Harel M, Grinvald A. Relationship between intrinsic connections and functional architecture revealed by optical imaging and in vivo targeted biocytin injections in primate striate cortex. *Proc Natl Acad Sci U S A.* 1993;90(22):10469–10473.
10. Rockland KS, Lund JS, Humphrey AL. Anatomical binding of intrinsic connections in striate cortex of tree shrews (Tupaia glis). *J Comp Neurol.* 1982;209(1):41–58.
11. Stettler DD, Das A, Bennett J, Gilbert CD. Lateral connectivity and contextual interactions in macaque primary visual cortex. *Neuron.* 2002;36(4):739–750.

12. Ts'o DY, Gilbert CD, Wiesel TN. Relationships between horizontal interactions and functional architecture in cat striate cortex as revealed by cross-correlation analysis. *J Neurosci.* 1986;6(4):1160–1170.
13. Weliky M, Kandler K, Fitzpatrick D, Katz LC. Patterns of excitation and inhibition evoked by horizontal connections in visual cortex share a common relationship to orientation columns. *Neuron.* 1995;15(3): 541–552.
14. Angelucci A, Levitt JB, Walton EJ, Hupe JM, Bullier J, Lund JS. Circuits for local and global signal integration in primary visual cortex. *J Neurosci.* 2002;22(19):8633–8646.
15. Cavanaugh JR, Bair W, Movshon JA. Nature and interaction of signals from the receptive field center and surround in macaque V1 neurons. *J Neurophysiol.* 2002;88(5):2530–2546.
16. Hashemi-Nezhad M, Lyon DC. Orientation tuning of the suppressive extraclassical surround depends on intrinsic organization of V1. *Cereb Cortex.* 2012;22(2):308–326.
17. Sceniak MP, Ringach DL, Hawken MJ, Shapley R. Contrast's effect on spatial summation by macaque V1 neurons. *Nat Neurosci.* 1999;2(8): 733–739.
18. Das A, Gilbert CD. Topography of contextual modulations mediated by short-range interactions in primary visual cortex. *Nature.* 1999; 399(6737):655–661.
19. Liu YJ, Hashemi-Nezhad M, Lyon DC. Sharper orientation tuning of the extraclassical suppressive-surround due to a neuron's location in the V1 orientation map emerges late in time. *Neuroscience.* 2013;229: 100–117.
20. Nauhaus I, Benucci A, Carandini M, Ringach DL. Neuronal selectivity and local map structure in visual cortex. *Neuron.* 2008;57(5):673–679.
21. Gilbert CD. Horizontal integration and cortical dynamics. *Neuron.* 1992;9(1):1–13.
22. Seriès P, Lorenceau J, Frégnac Y. The "silent" surround of V1 receptive fields: theory and experiments. *J Physiol Paris.* 2003;97(4–6): 453–474.
23. Sillito AM, Grieve KL, Jones HE, Cudeiro J, Davis J. Visual cortical mechanisms detecting focal orientation discontinuities. *Nature.* 1995;378(6556):492–496.
24. Zipser K, Lamme VA, Schiller PH. Contextual modulation in primary visual cortex. *J Neurosci.* 1996;16(22):7376–7389.
25. DeAngelis GC, Freeman RD, Ohzawa I. Length and width tuning of neurons in the cat's primary visual cortex. *J Neurophysiol.* 1994;71(1): 347–374.
26. Levitt JB, Lund JS. Contrast dependence of contextual effects in primate visual cortex. *Nature.* 1997;387(6628):73–76.
27. Liu YJ, Hashemi-Nezhad M, Lyon DC. Dynamics of extraclassical surround modulation in three types of V1 neurons. *J Neurophysiol.* 2011;105(3):1306–1317.
28. Sengpiel F, Sen A, Blakemore C. Characteristics of surround inhibition in cat area 17. *Exp Brain Res.* 1997;116(2):216–228.
29. Shushruth S, Nurminen L, Bijanzadeh M, Ichida JM, Vanni S, Angelucci A. Different orientation tuning of near- and far-surround suppression in macaque primary visual cortex mirrors their tuning in human perception. *J Neurosci.* 2013;33(1):106–119.
30. Ahmed B, Anderson JC, Douglas RJ, Martin KA, Nelson JC. Polyneuronal innervation of spiny stellate neurons in cat visual cortex. *J Comp Neurol.* 1994;341(1):39–49.
31. Anderson JC, Douglas RJ, Martin KA, Nelson JC. Synaptic output of physiologically identified spiny stellate neurons in cat visual cortex. *J Comp Neurol.* 1994;341(1):16–24.
32. Hirsch JA, Gilbert CD. Synaptic physiology of horizontal connections in the cat's visual cortex. *J Neurosci.* 1991;11(6):1800–1809.
33. Kisvárday ZF, Tóth E, Rausch M, Eysel UT. Orientation-specific relationship between populations of excitatory and inhibitory lateral connections in the visual cortex of the cat. *Cereb Cortex.* 1997;7(7):605–618.
34. Angelucci A, Bressloff PC. Contribution of feedforward, lateral and feedback connections to the classical receptive field center and extraclassical receptive field surround of primate V1 neurons. *Prog Brain Res.* 2006;154:93–120.
35. Angelucci A, Bullier J. Reaching beyond the classical receptive field of V1 neurons: horizontal or feedback axons? *J Physiol Paris.* 2003;97(2–3):141–154.
36. Bullier J, Hupé JM, James AC, Girard P. The role of feedback connections in shaping the responses of visual cortical neurons. *Prog Brain Res.* 2001;134:193–204.
37. Levitt JB, Lund JS. The spatial extent over which neurons in macaque striate cortex pool visual signals. *Vis Neurosci.* 2002;19(4):439–452.
38. Cantone G, Xiao J, McFarlane N, Levitt JB. Feedback connections to ferret striate cortex: direct evidence for visuotopic convergence of feedback inputs. *J Comp Neurol.* 2005;487(3):312–331.
39. Schwabe L, Ichida JM, Shushruth S, Mangapathy P, Angelucci A. Contrast-dependence of surround suppression in Macaque V1: experimental testing of a recurrent network model. *Neuroimage.* 2010;52(3): 777–792.
40. Anderson JC, Martin AC. The synaptic connections between cortical areas V1 and V2 in macaque monkey. *J Neurosci.* 2009;29(36): 11283–11293.
41. Johnson P, Burkhalter A. Microcircuitry of forward and feedback connections within rat visual cortex. *J Comp Neurol.* 1996;368(3): 383–398.
42. Liu YJ, Ehrengruber MU, Negwer M, Shao HJ, Cetin AH, Lyon DC. Tracing inputs to inhibitory or excitatory neurons of mouse and cat visual cortex with a targeted rabies virus. *Curr Biol.* 2013;23(18): 1746–1755.
43. Fries W, Distel H. Large layer VI neurons of monkey striate cortex (Meynert cells) project to the superior colliculus. *Proc R Soc Lond B Biol Sci.* 1983;219(1214):53–59.
44. Fries W, Keizer K, Kuypers HG. Large layer VI cells in macaque striate cortex (Meynert cells) project to both superior colliculus and prestriate visual area V5. *Exp Brain Res.* 1985;58(3):613–616.
45. Hof PR, Glezer II, Nimchinsky EA, Erwin JM. Neurochemical and cellular specializations in the mammalian neocortex reflect phylogenetic relationships: evidence from primates, cetaceans, and artiodactyls. *Brain Behav Evol.* 2000;55(6):300–310.
46. Hof PR, Ungerleider LG, Webster MJ, et al. Neurofilament protein is differentially distributed in subpopulations of corticocortical projection neurons in the macaque monkey visual pathways. *J Comp Neurol.* 1996;376(1):112–127.
47. Rockland KS, Knutson T. Axon collaterals of Meynert cells diverge over large portions of area V1 in the macaque monkey. *J Comp Neurol.* 2001;441(2):134–147.
48. Kelly RM, Strick PL. Rabies as a transneuronal tracer of circuits in the central nervous system. *J Neurosci Methods.* 2000;103(1):63–71.
49. Lyon DC, Nassi JJ, Callaway EM. A disynaptic relay from superior colliculus to dorsal stream visual cortex in macaque monkey. *Neuron.* 2010;65(2):270–279.
50. Morimoto K, Hooper DC, Carbaugh H, Fu ZF, Koprowski H, Dietzschold B. Rabies virus quasispecies: implications for pathogenesis. *Proc Natl Acad Sci U S A.* 1998;95(6):3152–3156.
51. Ugolini G. Use of rabies virus as a transneuronal tracer of neuronal connections: implications for the understanding of rabies pathogenesis. *Dev Biol (Basel).* 2008;131:493–506.
52. Kelly RM, Strick PL. Cerebellar loops with motor cortex and prefrontal cortex of a nonhuman primate. *J Neurosci.* 2003;23(23):8432–8444.
53. Lyon DC, Rabideau C. Lack of robust LGN label following transneuronal rabies virus injections into macaque area V4. *J Comp Neurol.* 2012;520(11):2500–2511.
54. Nassi JJ, Lyon DC, Callaway EM. The parvocellular LGN provides a robust disynaptic input to the visual motion area MT. *Neuron.* 2006;50(2):319–327.
55. Wong-Riley M. Changes in the visual system of monocularly sutured or enucleated cats demonstrable with cytochrome oxidase histochemistry. *Brain Res.* 1979;171(1):11–28.
56. Brodmann K. *Vergleichende Lokalisationslehre der Grosshirnrinde* [*Comparative Localization Theory of the Cerebral Cortex*]. Leipzig: Barth; 1909. German.

57. Lyon DC. Morphological approaches to the anatomical dissection of neuronal circuits. In: Fellin T, Halassa M, editors. *Neuronal Network Analysis: Concepts and Experimental Approaches*. New York: Springer Science Humana Press; 2012:375–389.
58. Nhan HL, Callaway EM. Morphology of superior colliculus- and middle temporal area-projecting neurons in primate primary visual cortex. *J Comp Neurol.* 2012;520(1):52–80.
59. Van Essen DC, Newsome WT, Maunsell JH. The visual field representation in striate cortex of the macaque monkey: asymmetries, anisotropies, and individual variability. *Vision Res.* 1984;24(5):429–448.
60. Weller RE, Kaas JH. Retinotopic patterns of connections of area 17 with visual areas V-II and MT in macaque monkeys. *J Comp Neurol.* 1983;220(3):253–279.
61. Rockland KS. Bistratified distribution of terminal arbors of individual axons projecting from area V1 to middle temporal area (MT) in the macaque monkey. *Vis Neurosci.* 1989;3(2):155–170.
62. Bair W, Cavanaugh JR, Movshon JA. Time course and time-distance relationships for surround suppression in macaque V1 neurons. *J Neurosci.* 2003;23(20):7690–7701.
63. Webb BS, Dhruv NT, Solomon SG, Tailby C, Lennie P. Early and late mechanisms of surround suppression in striate cortex of macaque. *J Neurosci.* 2005;25(50):11666–11675.
64. Bringuier V, Chavane F, Glaeser L, Frégnac Y. Horizontal propagation of visual activity in the synaptic integration field of area 17 neurons. *Science.* 1999;283(5402):695–699.
65. Girard P, Hupé JM, Bullier J. Feedforward and feedback connections between areas V1 and V2 of the monkey have similar rapid conduction velocities. *J Neurophysiol.* 2001;85(3):1328–1331.
66. Grinvald A, Lieke EE, Frostig RD, Hildesheim R. Cortical point-spread function and long-range lateral interactions revealed by real-time optical imaging of macaque monkey primary visual cortex. *J Neurosci.* 1994;14(5 Pt 1):2545–2568.
67. Alitto HJ, Usrey WM. Origin and dynamics of extraclassical suppression in the lateral geniculate nucleus of the macaque monkey. *Neuron.* 2008 10;57(1):135–146.
68. Bolz J, Gilbert CD. The role of horizontal connections in generating long receptive fields in the cat visual cortex. *Eur J Neurosci.* 1989;1(3):263–268.
69. Gilbert CD. Laminar differences in receptive field properties of cells in cat primary visual cortex. *J Physiol.* 1977;268(2):391–421.
70. Henry CA, Joshi S, Xing D, Shapley RM, Hawken MJ. Functional characterization of the extraclassical receptive field in macaque V1: contrast, orientation, and temporal dynamics. *J Neurosci.* 2013;33(14):6230–6242.
71. Sceniak MP, Hawken MJ, Shapley R. Visual spatial characterization of macaque V1 neurons. *J Neurophysiol.* 2001;85(5):1873–1887.
72. Shushruth S, Ichida JM, Levitt JB, Angelucci A. Comparison of spatial summation properties of neurons in macaque V1 and V2. *J Neurophysiol.* 2009;102(4):2069–2083.
73. Allison JD, Casagrande VA, Bonds AB. The influence of input from the lower cortical layers on the orientation tuning of upper layer V1 cells in a primate. *Vis Neurosci.* 1995;12(2):309–320.
74. Bolz J, Gilbert CD. Generation of end-inhibition in the visual cortex via interlaminar connections. *Nature.* 1986;320(6060):362–365.
75. Eyding D, Macklis JD, Neubacher U, Funke K, Wörgötter F. Selective elimination of corticogeniculate feedback abolishes the electroencephalogram dependence of primary visual cortical receptive fields and reduces their spatial specificity. *J Neurosci.* 2003;23(18):7021–7033.
76. Olsen SR, Bortone DS, Adesnik H, Scanziani M. Gain control by layer six in cortical circuits of vision. *Nature.* 2012;483(7387):47–52.
77. Grieve KL, Sillito AM. A re-appraisal of the role of layer VI of the visual cortex in the generation of cortical end inhibition. *Exp Brain Res.* 1991;87(3):521–529.
78. Thomson AM. Neocortical layer 6, a review. *Front Neuroanat.* 2010;4:13.
79. Movshon JA, Newsome WT. Visual response properties of striate cortical neurons projecting to area MT in macaque monkeys. *J Neurosci.* 1996;16(23):7733–7741.
80. Albright TD, Desimone R, Gross CG. Columnar organization of directionally selective cells in visual area MT of the macaque. *J Neurophysiol.* 1984;51(1):16–31.
81. Felleman DJ, Kaas JH. Receptive-field properties of neurons in middle temporal visual area (MT) of owl monkeys. *J Neurophysiol.* 1984;52(3):488–513.
82. Sherwood CC, Lee PW, Rivara CB, et al. Evolution of specialized pyramidal neurons in primate visual and motor cortex. *Brain Behav Evol.* 2003;61(1):28–44.
83. Lyon DC, Kaas JH. Evidence for a modified V3 with dorsal and ventral halves in macaque monkeys. *Neuron.* 2002;33(3):453–461.
84. Hassler R. Comparative anatomy in the central visual systems in day- and night-active primates. In: Hassler R, Stephan H, editors. *Evolution of the Forebrain*. Springer Science + Business Media, New York; 1966:419–434.

Eye and Brain

Dovepress

Publish your work in this journal

Eye and Brain is an international, peer-reviewed, open access journal focusing on clinical and experimental research in the field of neuro-ophthalmology. All aspects of patient care are addressed within the journal as well as basic research. Papers covering original research, basic science, clinical and epidemiological studies, reviews and evaluations, guidelines, expert opinion and commentary, case reports and extended reports are welcome. The manuscript management system is completely online and includes a very quick and fair peer-review system, which is all easy to use. Visit http://www.dovepress.com/testimonials.php to read real quotes from published authors.

Submit your manuscript here: http://www.dovepress.com/eye-and-brain-journal